Comparative EPR and Redox Studies of Three Prokaryotic Enzymes of the Xanthine Oxidase Family: Quinoline 2-Oxidoreductase, Quinaldine 4-Oxidase, and Isoquinoline 1-Oxidoreductase†

Christoph Canne,‡ Ingrid Stephan,§ Jürgen Finsterbusch,‡ Franz Lingens,§ Reinhard Kappl,‡ Susanne Fetzner,|| and Jürgen Hüttermann*,‡

Fachrichtung Biophysik und Physikalische Grundlagen der Medizin, Universität des Saarlandes, Klinikum Geb. 76, D-66421 Homburg/Saar, Germany, Institut für Mikrobiologie der Universität Hohenheim, Garbenstr. 30, D-70593 Stuttgart, Germany, and Fachbereich 7-Biologie, Carl von Ossietzky Universität Oldenburg, Postfach 2503, D-26111 Oldenburg, Germany

Received March 13, 1997; Revised Manuscript Received June 11, 1997⊗

ABSTRACT: For three prokaryotic enzymes of the xanthine oxidase family, namely quinoline 2-oxidoreductase, quinaldine 4-oxidase, and isoquinoline 1-oxidoreductase, the electron transfer centers were investigated by electron paramagnetic resonance. The enzymes are containing a molybdenum-molybdopterin cytosine dinucleotide cofactor, two distinct [2Fe-2S] clusters and, apart from isoquinoline 1-oxidoreductase, a flavin adenine dinucleotide. The latter cofactor yields two different organic radical signals in quinoline 2-oxidoreductase and quinaldine 4-oxidase, typical for the neutral and anionic form, respectively. A "rapid" Mo(V) species is present in all enzymes with small differences in magnetic parameters. From spectra simulation of ^{95}Mo-substituted quinoline 2-oxidoreductase, a deviation of 25° between the maximal **g** and ^{95}Mo-hyperfine tensor component was derived. The very rapid Mo(V) species was detected in small amounts upon reduction with substrates in quinoline 2-oxidoreductase and quinaldine 4-oxidase, but showed a different kinetic behavior with considerable EPR intensities in isoquinoline 1-oxidoreductase. The FeSI and FeSII centers produced different signals in all three enzymes and, in case of isoquinoline 1-oxidoreductase, revealed a dipolar interaction, from which a maximum distance of 15 Å between FeSI and FeSII was estimated. The midpoint potentials of the FeS centers were surprisingly different and determined for FeSI/FeSII with −155/−195 mV in quinoline 2-oxidoreductase, −250/−70 mV in quinaldine 4-oxidase, and +65/+10 mV in isoquinoline 1-oxidoreductase. The slopes of the fitting curves for the Nernst equation are indicative for nonideal behavior. Only in quinoline 2-oxidoreductase, an averaged midpoint potential of the molybdenum redox pairs of about −390 mV could be determined. Both of the other enzymes did not produce Mo(V) signals in redox titration experiments, probably because of direct reduction of Mo(VI) to Mo(IV) in the presence of dithionite.

Enzymes containing a pterin molybdenum cofactor are ubiquitous in organisms and are involved in important biological processes (Bray & Swann, 1972; Bray, 1975, 1980, 1988; Coughlan, 1980; Gutteridge & Bray, 1980a; Cramer, 1983; Hille & Massey, 1985; Bray et al., 1991; Pilato & Stiefel, 1993; Hille, 1994, 1996). On the basis of the structures of their molybdenum centers, these enzymes have been categorized into three families: the xanthine oxidase family, the sulfite oxidase family, and the dimethylsulfoxide reductase family (Hille, 1996). The establishment of these three principle families has also been justified by recent studies investigating amino acid sequence homologies among known molybdenum-containing enzymes (Lehmann et al., 1995; Bläse et al., 1996; Hille, 1996). Within the molybdenum-containing enzymes that belong to the xanthine oxidase family, the molybdenum hydroxylases catalyze the hydroxylation of their substrates in the presence of an electron acceptor. The oxygen atom incorporated into the respective product originates from water.

As an organic part of the molybdenum cofactor, molybdopterin and several dinucleotide forms of the pterin molybdenum cofactor have been described. Xanthine oxidase and xanthine dehydrogenases, for instance, were reported to contain molybdopterin. In carbon monoxide dehydrogenases from carboxidotrophic bacteria, in aldehyde oxidoreductase from *Desulfovibrio gigas*, and in the bacterial enzymes catalyzing the hydroxylation of quinoline or quinoline-derivatives, molybdopterin cytosine dinucleotide was found [for a survey, see Hille (1996)]. Apart from their distinct pterin molybdenum cofactor, most molybdenum hydroxylases contain two [2Fe-2S] clusters and flavin adenine dinucleotide. Some hydroxylases, however, lack the flavin cofactor.

For quinoline 2-oxidoreductase, a molybdo iron sulfur flavoprotein belonging to the xanthine oxidase family, we

† This work was supported by grants from the Deutsche Forschungsgemeinschaft (DFG), Grants Hu 248/11-1 and Li 78/35-1.

* To whom correspondence should be addressed.
‡ Universität des Saarlandes.
§ Institut für Mikrobiologie der Universität Hohenheim.
|| Carl von Ossietzky Universität Oldenburg.

⊗ Abstract published in *Advance ACS Abstracts,* August 1, 1997.

[1] Abbreviations: EPR, electron paramagnetic resonance; QuinOr, quinoline 2-oxidoreductase; QualOx, quinaldine 4-oxidase; IsoOr, isoquinoline 1-oxidoreductase; XanOx, xanthine oxidase; FeSI, less anisotropic iron-sulfur center; FeSII, more anisotropic iron-sulfur center; FAD, flavin adenine cofactor; Tris-HCl, Tris(hydroxymethyl)aminomethanehydrochloride.

S0006-2960(97)00581-3 CCC: $14.00

have presented a first EPR[1] study of its various paramagnetic redox centers in a recent paper (Tshisuaka et al., 1993). Several Mo(V) species were described and, for convenience, were named in an analogous way like comparable signals in well characterized enzymes, such as xanthine oxidase (XanOx) from cow's milk (Bray, 1980; Hille, 1994). To indicate unique spectral properties typical for quinoline 2-oxidoreductase, the extension "q" was added. A rapid q signal is readily induced upon addition of substrate exhibiting a single proton hyperfine coupling due to the reduction of a sulfido group to a sulfhydryl group at the molybdenum center. In addition, a resting q signal, always present in very small amounts in the samples as isolated, was assigned to an inactive form of the Mo(V) center. In the cyanide inactivated (desulfo) dioxo form of the molybdenum cofactor, a slow q signal was detected for which tentatively a proton interaction was discussed. Apart from Mo(V) signals, an organic radical signal with a **g** factor and a line width typical for the neutral form of the flavin adenine dinucleotide (FAD) cofactor was observed, but another origin for this signal, e.g., the pterin cofactor, could not be ruled out. The signals of the two distinct [2Fe-2S] clusters, visible only at temperatures below 60 K, were designated FeSI (with smaller **g** anisotropy) and FeSII (with larger **g** anisotropy) according to the convention in literature (Bray, 1975; Bray et al., 1991).

In this paper we wish to present results of EPR studies of isoquinoline 1-oxidoreductase (IsoOr) and quinaldine 4-oxidase (QualOx), two further molybdenum hydroxylases belonging to the xanthine oxidase family. QualOx resembles QuinOr with respect to its complex structure $\alpha_2\beta_2\gamma_2$ and its cofactor composition, but differs in its substrate and electron acceptor specificity (Stephan et al., 1996). In contrast, IsoOr from *Pseudomonas diminuta* 7 is a heterodimeric molybdo iron-sulfur enzyme lacking the flavin cofactor. Purification and characterization of both enzymes were described in earlier papers (Lehmann et al., 1994; Stephan et al., 1996).

In order to characterize the three hydroxylases, redox potentials of their molybdenum cofactors and their [2Fe-2S] clusters were measured under anaerobic conditions by potentiometric titration with sodium dithionite in Tris-buffered solutions. In order to reveal magnetic hyperfine parameters more precisely, EPR spectra of ^{95}Mo-QuinOr were recorded.

MATERIALS AND METHODS

Preparation of Enzyme Samples. QuinOr was purified from *Pseudomonas putida* 86 grown on quinoline as sole source of carbon and energy. IsoOr was prepared from the isoquinoline degrading strain *P. diminuta* 7, and QualOx was purified from *Arthrobacter* sp. Rü61a, which utilizes quinaldine (2-methylquinoline) as carbon source. Details of bacterial growth and enzyme purification have been described previously (Tshisuaka et al., 1993; Lehmann et al., 1994; Stephan et al., 1996). ^{95}Mo-enriched QuinOR was prepared in an analogous way from *P. putida* 86 grown in mineral salt medium that contained 0.01 g/L (^{95}Mo)-sodium molybdate ($Na_2MoO_4 \times 2\ H_2O$) [isotope purchased from Campro Scientific (Emmerich/Germany) with 95.5% purity]. Homogeneity of the preparations was tested by gel electrophoresis and by UV−vis spectroscopy recording the ratio E280/E450 nm for which a value of 4.0 (QuinOr), 5.0 (QualOx), and 8.0 (IsoOr) was taken as a criterion of purity. The activity was assayed by following the substrate dependent reduction of the monotetrazolium salt *p*-iodonitrotetrazolium violet (INT) to its formazan as described previously (Bauder et al., 1990; Lehmann et al., 1994; Stephan et al., 1996).

Preparation of EPR Samples. For reduction, 1 μL of substrate (340 mM in ethanol) or 10 μL of 0.1 M or 0.2 M $Na_2S_2O_4$ were added to approximately 30 nmol of native enzyme in 200 μL of 100 mM Tris-HCl, pH 8.0, and the samples were transferred into quartz tubes and frozen in liquid nitrogen within 1 min. The dithionite reduced samples were repeatedly thawed under nitrogen atmosphere, incubated at room temperature, frozen, and re-examined by EPR. Desulfo samples were prepared analogous to desulfo XanOx, according to Massey and Edmondson (1970) and Gutteridge et al. (1978b). QuinOr (90 nmol/mL) was incubated for 180 min at room temperature with KCN at final concentrations of up to 12.5 mM. The enzyme was thoroughly washed with buffer and concentrated by ultrafiltration. The samples (31 nmol in 200 μL buffer), less than 0.5% functional, were reduced with substrate and dithionite as described above and frozen in nitrogen within 1 min. After recording the EPR spectra, the samples were thawed, further incubated at room temperature for 10 min, reinvestigated by EPR, and so on, so that finally EPR spectra for 1, 10, 20, 30, and 45 min after addition of reductant were obtained. QualOx and IsoOr were treated in a similar way.

Redox Titrations. Redox titrations of the enzymes were carried out in 0.2 M Tris-HCl buffer, pH 8.0, under strictly anaerobic conditions. The titration vessel was installed in an anaerobic chamber, filled with a nitrogen (95%)−hydrogen (5%) gaseous mixture, and stirred under argon gas, purified by oxygen adsorbants (Messer Griesheim, Oxysorb). The redox potential was measured by a combined micro platinum electrode (Metrohm 6.0408.100) with a Ag/AgCl reference, calibrated against a saturated quinhydrone solution, pH 7.0. The redox potential of the system was adjusted with small additions of 0.01 or 0.1 M solutions of $Na_2S_2O_4$ or $K_3[Fe(CN)_6]$. The total time for a titration was in almost all cases about 2 h. After equilibration for about 5 min, 250 μL of the solution was filled into EPR tubes and immediately frozen in liquid nitrogen. In order to obtain stable potentials, the following mediators were used (midpoint potentials at pH 7): 2,6-dichloroindophenol (217 mV), 1,2-naphthoquinone (145 mV), phenazine methosulfate (80 mV), 1,4-naphthoquinone (60 mV), toluidine blue (31 mV), potassium indigotetrasulfonate (−46 mV), indigocarmine (−125 mV), 2-hydroxynaphthoquinone (−145 mV), anthraquinone-1,5-disulfonate (−170 mV), anthraquinone-2-sulfonate (−225 mV), phenosafranine (−252 mV), safranine T (−289 mV), benzyl viologen (−311 mV), diquat dibromide (−350 mV), methyl viologen (−440 mV) and ethyl viologen (−440 mV). Diquat dibromide was supplied by Promochem (Wesel, Germany), all the others were purchased from Sigma/Aldrich.

Mo(V) EPR spectra were recorded at 77 K and the reduced iron-sulfur signals at 25 K. All samples were measured at a defined position within the EPR cavity at nearly identical microwave frequencies. The redox measurements were reproduced three times for QuinOr and twice for IsoOr and QualOx.

Simulation of the Titration Curves. In order to obtain the midpoint potentials for the FeS centers, the relative intensities of the following components of the rhombic iron-sulfur signals were plotted against the measured redox potential: QuinOr, g_1, g_3 (FeSI and FeSII); IsoOr, g_2, g_3 (FeSI), and

g_1, g_2 (FeSII) and QualOx, g_3 (FeSI) and g_1, g_2, and g_3 (FeSII).The fit of data points was achieved using the Nernst equation in a rearranged form:

$$E = E_M + f_N \log_{10}\left(\frac{1}{\kappa} - 1\right)$$

with κ as the degree of reduction of FeS centers, f_N the Nernst-factor (59 mV for $n = 1$), and E_M the midpoint potential (at pH 8.0), where equal concentrations of reduced and oxidized FeS clusters are present.

The Mo(V) signals were evaluated by determining the amplitudes of the $\mathbf{g}_\perp$ feature of the rapid q signal for the various redox potentials since an integration was not feasible due to the presence of variable amounts of mediator radical signals. For the two reduction steps of the Mo center, the equation

$$\kappa = \frac{[Mo^V]}{[Mo^{total}]} = \left[\exp\left(\frac{2.303}{f_N}E\right)\exp\left(\frac{2.303}{f_N}E_M\right)\right] \Big/ \left[\exp\left(\frac{2.303}{f_N}2E\right) + \exp\left(\frac{2.303}{f_N}E\right)\exp\left(\frac{2.303}{f_N}E_M\right) + \exp\left(\frac{2.303}{f_N}2E_M\right)\right]$$

was used to fit the redox behavior of the Mo(V) center (Cammack, 1994), assuming that the individual midpoint potentials of each reduction step of the Mo center are close to the averaged midpoint potential $E_M = 0.5(E^{Mo(VI)/Mo(V)} + E^{Mo(V)/Mo(IV)})$.

For all fits of the titration curves of the FeS centers, the ideal behavior ($f_N = 59$ mV) was statistically examined by applying an F test to the regressor f_N to check, whether the hypothesis $f_N = 59$ (mV) can be rejected. This is the case if

$$\left(\frac{\hat{f} - 59}{\hat{\sigma}_{\hat{f}_N}}\right)^2 \geq F(1 - \alpha; n)$$

[$\hat{f}_N$, general least-square estimation; $\hat{\sigma}_{\hat{f}_N}^2$, variance of $\hat{f}_N$; F, in statistical tables listed F value to the significance level ($1 - \alpha$) and the degrees of freedom n]. For every fit, the P value, which denotes the smallest probability for which the hypothesis $f_N = 59$ (mV) could be rejected, was calculated. For a given significance level α (we have used 0.05), the hypothesis must be rejected, if the P value is smaller than α. If the P value exceeds α, then the statistical test remains insignificant.

In order to simulate nonideal behavior of the FeS centers ($f_N > 59$ mV), the Nernst equation was modified in such a way, that a Gaussian distribution of midpoint potentials was taken into account. The equation is then given by:

$$\kappa(E,\sigma) = \int_{-\infty}^{+\infty} N(E_M,\sigma)\kappa(E,E_M)\mathrm{d}E_M = \frac{1}{\sqrt{2\pi\sigma^2}} \times \int_{-\infty}^{+\infty} \exp\left(-\frac{E_M^2}{2\sigma^2}\right) \frac{\exp\left(\frac{2.303}{f_N}E\right)}{\exp\left(\frac{2.303}{f_N}E\right) + \exp\left(\frac{2.303}{f_N}E_M\right)} \mathrm{d}E_M$$

[with $N(E_M,\sigma)$, the normal distribution with the expectation value E_M and the standard deviation σ].

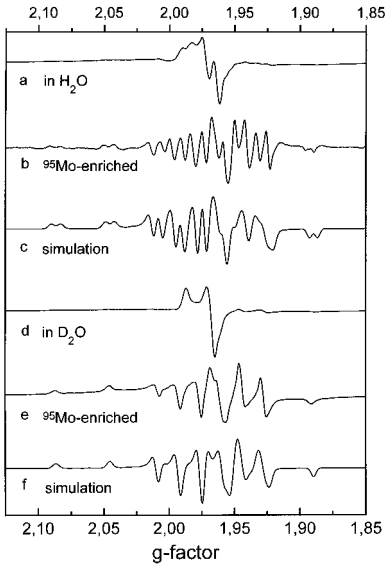

FIGURE 1: EPR spectra of QuinOr from *Pseudomonas putida* 86, (a and b) reduced with quinoline in H_2O, (d and e) reduced with quinoline in D_2O. Spectra b and e were obtained from ^{95}Mo-enriched samples in H_2O and D_2O, spectra c and f show simulations with the parameters given in Table 1. Spectra were recorded at 77 K, the modulation amplitude was 0.5 mT.

EPR Spectroscopy. EPR spectra at X-band frequencies were recorded on Bruker ER 420 or ESP 300 spectrometers equipped with a continuous helium flow cryostat (ESR 900, Oxford Instruments) for the temperature range from 4 to 60 K or with a quartz dewar for measurements at liquid nitrogen temperature. The magnetic field and the microwave frequency were determined with a NMR gaussmeter and a microwave counter, respectively. The modulation amplitude for spectra recording generally was 0.5 mT; for spectra of the redox titrations, 0.4 mT modulation amplitude and 12.5 mW microwave power were used. The Q-band spectra were recorded on a Bruker ER 220 spectrometer in a temperature range from 10 to 50 K (CF 935 cryostat, Oxford Instruments), using a modulation amplitude of 0.6 mT. The microwave power typically was 5 mW.

For simulation of the Mo(V) powder spectra, either the modified QCPE program MSPOWD, which diagonalizes the complete Hamiltonian including quadrupolar tensors, or the home made program IWASAKI, based on the formalism developed by Iwasaki (1974), was used.

RESULTS

EPR Spectra of Quinoline 2-Oxidoreductase. The EPR spectrum of the enzyme in aqueous buffer reduced with the substrate quinoline shows the apparently axial pattern of the rapid q species with the doublet splitting of a single proton (Figure 1a), which was assigned to the proton at the sulfido group of the reduced molybdenum center (Tshisuaka et al., 1993). The hyperfine interaction is lost upon substitution of H_2O with D_2O, revealing a spectrum with axial **g** symmetry (Figure 1d). Rapid q species were also found after addition of the substrate analogues quinoxaline, quinazoline, or 8-methylquinoline to QuinOr, with generally lower intensities but otherwise identical **g** and hyperfine parameters.

To gain further information on the molybdenum nucleus, EPR spectra of ^{95}Mo-enriched samples were recorded (Figure 1, spectra b and e), in which the hyperfine interaction leads to a 6-fold splitting of the lines due to the nuclear spin $I = {}^5/_2$ in addition to the doublet proton splitting in aqueous

Table 1: EPR Parameters[a,b] of Mo(V) Centers and FAD Radicals

center[c]	quinoline 2-oxidoreductase	quinaldine 4-oxidase	isoquinoline 1-oxidoreductase
very rapid	$\mathbf{g}_1$: 2.0244, $\mathbf{g}_2$: 1.9576, $\mathbf{g}_3$: 1.9500	$\mathbf{g}_1$: 2.0243, $\mathbf{g}_2$: 1.945, $\mathbf{g}_3$: 1.935	$\mathbf{g}_1$: 2.0243, $\mathbf{g}_2$: 1.9545, $\mathbf{g}_3$: 1.9411
rapid	$\mathbf{g}_1$: 1.9880, $\mathbf{g}_2$: 1.9679, $\mathbf{g}_3$: 1.9650	$\mathbf{g}_{\|}$: 1.992, $\mathbf{g}_{\perp}$: 1.966	$\mathbf{g}_1$: 1.9900, $\mathbf{g}_2$: 1.9693, $\mathbf{g}_3$: 1.9601
	(^{1}H) $\mathbf{A}_{\|}$: 1.08, $\mathbf{A}_{\perp}$: 1.36 (quin), 1.15 (dith)	*e*	(^{1}H) $\mathbf{A}_1$: 1.33, $\mathbf{A}_2$: 1.75, $\mathbf{A}_3$: 1.70
	(^{95}Mo) $\mathbf{A}_1$: 6.57,[d] $\mathbf{A}_2$: 2.85,[d] $\mathbf{A}_3$: 2.70[d]		
resting	$\mathbf{g}_1$: 1.9885, $\mathbf{g}_2$: 1.9765, $\mathbf{g}_3$: 1.9537	not detected	not detected
resting 2	$\mathbf{g}_1$: 1.9911, $\mathbf{g}_2$: 1.9697, $\mathbf{g}_3$: 1.9630		
	(^{95,97}Mo) $\mathbf{A}_1$: 5.7, $\mathbf{A}_2$: 2.8, $\mathbf{A}_3$: nr		
slow	$\mathbf{g}_1$: 1.9663, $\mathbf{g}_2$: 1.9656, $\mathbf{g}_3$: 1.9581	not investigated	not detected
	(^{1}H) $\mathbf{A}_1$: 1.60, $\mathbf{A}_2$: 1.65, $\mathbf{A}_3$: 1.70		
FAD	**g**: 2.0034	**g**: 2.004	not present
	LW: 1.91	LW: 1.60	

[a] The parameters for QuinOr and IsoOr have been verified by simulation of the EPR spectra and the values for QualOx are the apparent values. [b] The hyperfine values **A** are given in millitesla, nr means not resolved, LW is the line width in millitesla. [c] The nomenclature for the centers was adopted from analogies to other enzymes, e.g., xanthine oxidase. [d] **g** and **A** tensor are noncoaxial (25° between the maximal components). [e] Poorly resolved splittings could not be related to an exchangeable proton so far.

solutions. The good agreement between experimental and simulated patterns (Figure 1, spectra c and f) was achieved with the parameters listed in Table 1, i.e., with a slightly rhombic **g** tensor for the rapid q species, a rhombic ^{95}Mo hyperfine coupling, and an axial proton **A** tensor. In comparison with our previous report (Tshisuaka et al., 1993) the **g** and **A** values can now be given with a higher precision. For the simulation, it was necessary to introduce a noncollinearity of 25° between the $\mathbf{g}_1$ and $\mathbf{A}_1$ tensor (^{95}Mo) components.

Additionally, it was found that also reduction with dithionite induces the rapid q Mo(V) species. A close inspection of this rapid signal (not shown) reveals a small difference in the proton $\mathbf{A}_{\perp}$ hyperfine values, which, by simulation, were determined with 1.15 mT for the dithionite reduced signal versus 1.36 mT for the substrate reduced signal. The $\mathbf{A}_{\|}$ proton coupling as well as the **g** values remained essentially identical (data shown in Table 1). Addition of substoichiometric amounts of substrate quinoline to QuinOr did not produce the rapid q signal.

In samples reduced with an excess of quinoline and frozen quickly (<20 s), besides the rapid q signal, a small spectral feature at $g = 2.024$ is visible (Figure 2a), which so far has not been observed. When the solution is allowed to react for 2 more minutes the feature has clearly decreased in intensity and is completely lost after a prolonged reaction time (>4 min). This apparent **g** factor is typical for the intermediate very rapid species found in XanOx (2.025, 1.954, 1.949) (Bray et al., 1979; Gutteridge & Bray, 1980b). Even though a sample in D_2O (without proton splitting) was used, the other **g** components could not clearly be resolved and are hidden in the flank of the rapid q signal as indicated by the arrows. When QuinOr is incubated with the quinoline derivative quinaldine, which is not a substrate converted by QuinOr, only the resting species is observable. Subsequent addition of quinoline to this sample leads to the appearance of the rapid q species and the FAD radical (see below) within 2 min. Besides these patterns, again a signal at $g = 2.024$ is present in considerable amounts [marked with an asterisk (*) in Figure 2b]. After 4 min, this signal and the FAD signal have decayed while the rapid q species increased by a factor of 2 (Figure 2c). Subtracting the latter spectrum to minimize the rapid q contributions (denoted with r) produces the pattern in Figure 2d which contains FAD and the additional features correlated to the $\mathbf{g} = 2.024$ line. A simulation of these rhombic features (Figure 2e) yields **g** factors of 2.0244, 1.9576, and 1.9500, which are remarkably similar to the values for the very rapid species in XanOx supporting the assignment to this species in QuinOr (parameters are listed in Table 1).

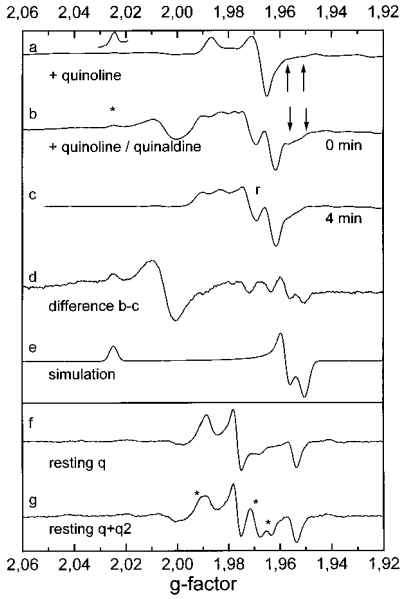

FIGURE 2: EPR spectra of QuinOr (a−e) showing traces of a "very rapid q" species. Spectrum a was obtained from samples in D_2O reduced with an excess of quinoline, the peak at $g = 2.024$ and the arrows indicating the very rapid q species, spectra b and c were recorded immediately and 4 min after addition of a mixture of quinoline and quinaldine in H_2O; (d) is the difference spectrum (b − c) with remainders of the Mo(V) rapid q signal (marked with r in spectrum c). Spectrum e shows a simulation of the very rapid q species with parameters of Table 1. EPR spectra (f, g) of two different resting signals of QuinOr associated with nonfunctional Mo(V) species. Spectrum f shows the resting q signal of the enzyme as isolated, spectrum g is obtained in cyanide-treated desulfo form after incubation with quinoline. In addition to the resting q signal a second resting q2 signal is apparent, for which simulation parameters are given in Table 1. All spectra were recorded at 77 K with 0.5 mT modulation amplitude.

The flavin adenosine dinucleotide (FAD) or the molybdopterin dinucleotide cofactor of QuinOr have been discussed as possible origins of the free radical (Tshisuaka et al., 1993). The EPR parameters (Table 1) suggest a neutral blue flavin radical (FADH$^{\bullet}$). Neither of the candidates could be ruled out, since removal of the FAD denatures the enzyme. Support for the assignment to FAD comes from experiments on the related enzyme IsoOr, which also contains two [2Fe-2S] centers and a molybdopterin dinucleotide cofactor but no FAD. In this enzyme, under no experimental conditions

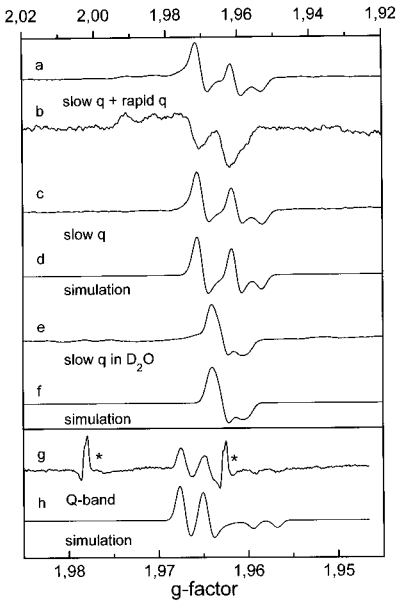

FIGURE 3: EPR spectra of cyanide-treated desulfo QuinOr after reduction with sodium dithionite. Spectrum a shows the slow q species with small contributions of the rapid q indicated in spectrum b. In spectrum c, rapid q contributions are eliminated yielding the pure slow q species for samples in H_2O and in spectrum e for samples in D_2O. Spectra d and f are the corresponding simulations of spectra c and e with parameters of Table 1. The Q-band spectrum of the slow q species in aqeous solution (g) is compared to the simulation (h). All spectra were recorded at 77 K, the Q-band spectrum is distorted by cavity contamination with manganese (*). Q-Band settings: modulation amplitude, 0.6 mT; microwave power, 5 mW.

is a free radical species observed. As can be inferred from Figure 2, spectra b and c, the FAD radical rapidly vanishes after addition of quinoline to the sample incubated with quinaldine. Since a fast and complete reoxidation by oxygen seems improbable, it is assumed that the FAD radical is converted to the reduced EPR-silent form.

Besides the rapid q and FAD signals present in active forms of the enzyme, some low intensity signals associated with nonfunctional Mo(V) species are observed for various preparations. The rhombic spectrum of the resting q Mo(V) species in the enzyme as isolated (Figure 2f) is compared with a spectrum of the desulfo form of the enzyme obtained after treatment with cyanide and incubation with the substrate quinoline (Figure 2g). The latter shows some additional lines of considerable intensity around $\mathbf{g} = 1.965$ together with a barely resolved spectral feature at $\mathbf{g}_1$, which are independent on incubation time. A close inspection of the resting q signal also reveals the presence of these lines at rather low intensity in this species. Subtracting the resting q signal from the desulfo signal renders a pattern, which is named resting q2 to distinguish it from the prevailing resting q signal in the as-prepared enzyme (contributions of resting q2 in Figure 2g marked with asterisks). Summation of simulated rhombic resting q2 and resting q species (parameters in Table 1) with a ratio of 1:1 provides a spectrum (not shown) closely resembling the experimental pattern of Figure 2g. It is noted that small and variable amounts of resting q2 species are found in different preparations, but larger amounts only appear in cyanide-treated desulfo samples with quinoline added.

When the desulfo enzyme is reduced with dithionite, a time-dependent increase of the slow q species is observed (Figure 3a). The spectrum was tentatively interpreted as rhombic with a resolved proton interaction (Tshisuaka et al., 1993). Careful studies of the slow q signals in various desulfo preparations using different cyanide concentrations indicated that the two low-field resonances are associated with a small concentration of the rapid q species. The corresponding spectrum (Figure 3b) was obtained by subtracting spectra of different desulfo samples annealed for 45 min after dithionite addition. Elimination of the rapid q contribution leaves a nearly axial slow q species with an exchangeable proton interaction (Figure 3, spectra c and d). The spectrum in H_2O was simulated with the parameters in Table 1, for D_2O the rescaled deuterium hyperfine interaction was used (Figure 3, spectra e and f). From the latter spectrum, the small deviation from axiality can be inferred. This result is corroborated by measurements at Q-band frequencies. The spectrum in H_2O, somewhat distorted by a cavity contamination with manganese, could be well reproduced with the parameters of Table 1 (Figure 3, spectra g and h).

The two distinct FeS species in QuinOr have been characterized in a recent publication (Tshisuaka et al., 1993). Their magnetic parameters are listed in Table 2 for comparison. In ^{57}Fe-substituted samples, no splittings due to the nuclear spin of $^1/_2$ were resolved, but the resonances are broadened (data not shown). The hyperfine interaction of the metal ions of both FeS clusters will be tackled by ENDOR spectroscopy.

Isoquinoline 1-Oxidoreductase. After reduction of IsoOr with an excess of sodium dithionite, a poorly resolved rhombic EPR signal is detected at 77 K, which sharpens for temperatures below 60 K (Figure 4a). It is assigned to an FeS cluster, which, on behalf of its characteristic **g** anisotropy, is called FeSI. For temperatures below 40 K, the signals of a second FeS center with larger **g** anisotropy (hence called FeSII) gradually become visible as indicated in Figure 4, spectra b and c. Its principal components are comparatively broad, the $\mathbf{g}_3$ component is overlapping with the corresponding feature of FeSI. Concomitantly, to the temperature-dependent appearance of the FeSII species, the $\mathbf{g}_1$ component of FeSI exhibits a reversible splitting in two peaks (I_{1a} and I_{1b}, Figure 4, spectra b and c), which are located symmetrically around the position of the original I_1 resonance. Q-band experiments (Figure 4e) clearly indicate that this splitting is not associated to a further **g** dominated species, because only one rhombic pattern corresponding to FeSI is observed. The splitting of the $\mathbf{g}_1$ component is hidden in the increased line width induced by pronounced **g** strain effects at the higher microwave frequency. Hence, in the absence of any Mo(V) species, a dipolar interaction between the two FeS centers has to be assumed. To check this assumption, a sample of IsoOr was reduced with an equimolar amount of dithionite. It does not produce signals of the FeSII species in detectable amounts nor a splitting of I_1 is observed at any temperature. The spectrum is identical to the pattern of the fully reduced sample at high temperature. For 25 mol of dithionite/mol of enzyme, signals I_a and I_b are superimposed on I_1 and a small amount of FeSII is discernible. Increasing the temperature to 50 K, the FeSII species and the splitting are vanishing. For a higher dithionite concentration of 50 mol/mol of enzyme, the signals I_{1a} and I_{1b} are more pronounced and FeSII is present in considerable amounts at 10 K. Because a further increase in dithionite concentration leaves the spectrum unchanged, the FeS centers are in a fully reduced state. Raising the

Table 2: EPR Parameters of the FeS Centers

enzyme	center	specification	$\mathbf{g}_1$ ($\mathbf{g}_{\|}$)	$\mathbf{g}_2$	($\mathbf{g}_{\perp}$)	$\mathbf{g}_3$	$\mathbf{g}_{av}$
quinoline 2-oxidoreductase	FeSI	reduced with dithionite	2.027	1.948		1.899	1.958
		reduced with quinoline	2.035	1.95[a]		1.898	1.961
	FeSII	reduced with dithionite	2.067	1.973		1.871	1.970
		reduced with quinoline	2.072	1.97[a]		1.866	1.969
quinaldine 4-oxidase	$FeSI_{ax}$		2.021		1.937		
	FeSII		2.075	1.983		1.874	1.977
isoquinoline 1-oxidoreductase	FeSI	$T > 50$ K or partial reduction	2.004	1.941		1.914	1.953
	FeSIa, Ib	$T < 30$ K and	2.013, 1.995[b]	1.944		1.916[b]	1.955
		full reduction, splitting[c]	3.0 mT	1.5 mT		1.5 mT	
	FeSI	$T < 30$ K and full reduction FeSII fully oxidized	2.010	1.945		1.919	1.958
	FeSII	$T = 20$ K	2.084	1.974		(<1.916)[d]	

[a] Values cannot be determined precisely due to superposition with Mo(V) signals. [b] Apparent values. [c] Inferred from simulation. [d] Value cannot be determined precisely due to extremely broad line and superposition with $\mathbf{g}_3$ of FeSI.

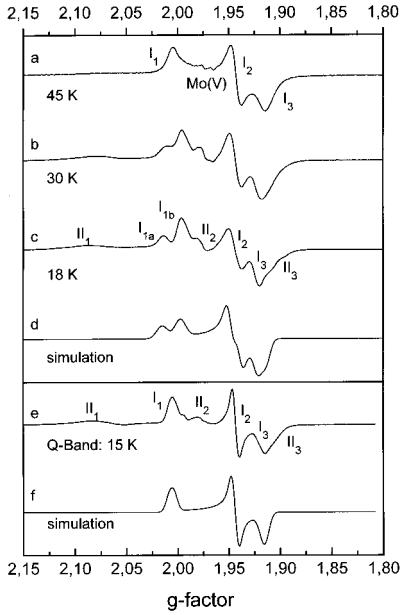

FIGURE 4: EPR spectra of the FeS centers of IsoOr from *Pseudomonas diminuta* 7, illustrating the coincidence of the rise of the FeSII signal and the appearance of the splitting of the g1 component of FeSI. Spectra a−c show a comparison of a fully reduced sample at different temperatures and trace e the Q-Band spectrum at 15 K. The low-temperature spectra (c, e) are compared to simulations, in which a zero-field splitting tensor was introduced (for parameters refer to Table 2). X-band spectra were recorded with 0.4 mT, Q-band spectra with 0.8 mT modulation amplitude.

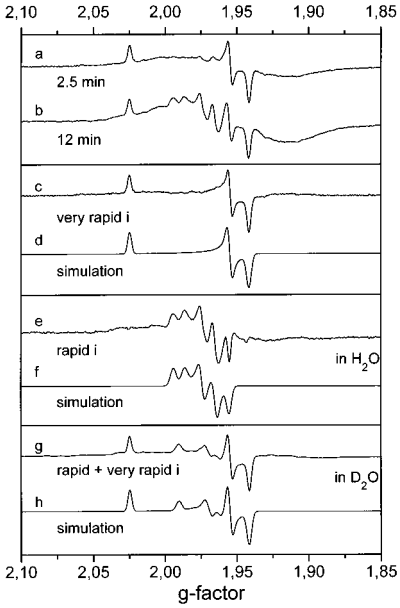

FIGURE 5: EPR spectra of IsoOr: spectrum a, 2.5 and spectrum b, 12 min after addition of substrate. Difference spectra show the very rapid i species (c), the rapid i species with exchangeable proton coupling (e), and both species in D_2O (g). The corresponding simulations with parameters listed in Table 1 are given in spectra d, f, and h. All spectra were recorded at 77 K with 0.5 mT modulation amplitude.

temperature to 50 K leads to the recurrence of a spectrum similar to that of Figure 4a. Splittings of $FeSI_2$ and $FeSI_3$ could not be resolved, but an increase of line widths is manifest. The effects of dipolar interaction between the centers were simulated for FeSI by introducing a small zero-field splitting tensor with the principal components D1, D2, D3 = 3.0, 1.5, and 1.5 mT, collinear with the **g** tensor. The simulated X-band pattern (Figure 4d) reproduces the characteristic features of the experimental spectrum. The Q-band simulation with identical parameters, compiled in Table 2, is given in Figure 4f. The splitting of the $\mathbf{g}_1$ resonance is not resolved due to the larger line width necessary in simulations (4.0 mT in Q-band vs 1.8 mT in X-band). The resonance designated II_2 appears at identical **g** factors in Q-band experiments (compare spectra c and e in Figure 4) and is not found in simulations, so that it is associated to the intermediate **g** component of FeSII.

In dithionite-reduced samples, only very small amounts of molybdenum-centered species could be detected in concentrated enzyme samples after extended spectra accumulation time. In contrast, Mo(V) signals could be readily monitored upon reduction with the substrate isoquinoline. Apart from broad FeSI signals, spectra at 77 K show different Mo(V) signals depending on the time elapsed between substrate addition and freezing (Figure 5, spectra a and b).

Shortly after substrate addition, a rhombic signal with large anisotropy, comparable to the very rapid signals of XanOx, was observed and will be called very rapid i. Its signal intensity grows for 5 min, then falls again, but the signal does not completely vanish even after 50 min of reaction time. These findings indicate, that the very rapid i species should be associated with an inhibited Mo(V) complex. A second, less anisotropic Mo(V) signal is at first hardly visible, rises for 10 min, and vanishes after that. Subsequent addition of substrate does not restore the signal. It shows a D_2O-exchangeable coupling (Figure 5g) and will be called rapid i because of its similarity to the rapid signal of XanOx.

The pure species can be isolated by numerical subtraction of spectra obtained after different incubation times with the substrate. The very rapid i spectrum is shown in Figure 5c together with the simulated pattern (Figure 5d), whose

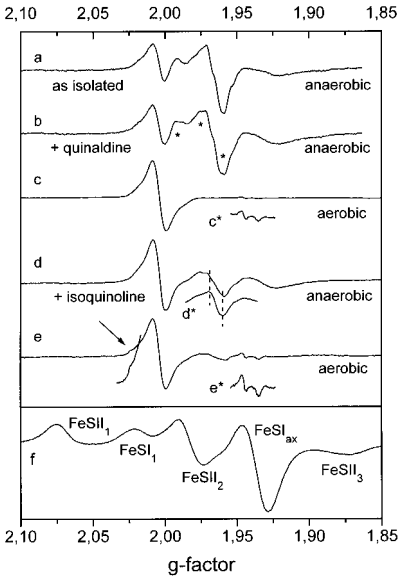

FIGURE 6: EPR signals of QualOx from *Arthrobacter* sp. Rü61a. (a) Signal of the organic FAD species together with a poorly resolved rapid species obtained from samples as isolated under anaerobic conditions, spectra b−c are spectra after addition of quinaldine, spectra d and e after addition of isoquinoline under anaerobic (b, d) and aerobic conditions (c, e). Signals of the reduced iron-sulfur centers are shown in spectrum f. Spectra a−e were recorded at 77 K, spectrum f at 35 K, both with 0.5 mT modulation amplitude.

simulation parameters are nearly identical to the corresponding species in XanOx and QuinOr (Table 1). The rapid i species presents a somewhat larger exchangeable proton hyperfine coupling (Figure 5, spectra e and f) and a more rhombic **g** tensor than QuinOr, which can be inferred from the spectra of the sample with D_2O exchanged buffer (Figure 5, spectra g and h). In the substrate-reduced enzyme, the rhombic signals of both FeS clusters are observed, which exhibit essentially the same behavior as in the dithionite reduced samples. Only the II_1-resonance exhibits a little larger apparent **g** value of 2.095. In cyanide-treated, desulfo IsoOr, iron-sulfur centers appear after reduction with dithionite. However, a slow-type Mo(V) signal like in QuinOr could not be obtained so far.

Quinaldine 4-Oxidase. The redox active centers of QualOx, which is related to QuinOr with respect to its molecular mass, subunit, and cofactor composition (Stephan et al., 1996), proved to be very sensitive to the oxygen status after preparation. The enzyme in the oxidized state (as isolated, aerobic conditions) did not elicit any EPR signals. Under anaerobic conditions, without substrate or reducing agent, at 77 K an EPR signal of an organic radical species at $\mathbf{g} = 2.0039$ was observed together with a rapid Mo(V) species, showing a poorly resolved splitting of ca. 0.9 mT, and a broad resonance around $\mathbf{g} = 1.925$, which arises from an iron-sulfur species (Figure 6a). When the substrate quinaldine is added to the anaerobically prepared sample, slight changes of the rapid signals are noticed (indicated by asterisks) while the other features are conserved (Figure 6b). Under aerobic conditions, the organic radical signal is drastically increased in intensity, whereas the rapid signal and the iron-sulfur resonances are completely lost (Figure 6c). Some weak features at $\mathbf{g} = 1.945$ and 1.935 are discernible, which are enhanced in trace c*. A line width of 1.6 mT is determined for the organic signal, which is characteristic for the anionic (red) flavin radical. It is noted, that for QuinOr and eukaryotic XanOx the presence of a neutral (blue) FAD radical species was derived (Palmer et al., 1971; Tshisuaka et al., 1993). Apart from quinaldine, the enzyme converts a number of other substrates like quinoline, quinoline derivatives substituted in position 2 and/or 8, or quinazoline as well as isoquinoline with high relative activity (Stephan et al., 1996). Therefore, EPR spectra after incubation with alternative substrates quinoline, 2-chloroquinoline, and isoquinoline under aerobic and anaerobic conditions were recorded. Spectra d and e of Figure 6 with isoquinoline added under anaerobic and aerobic conditions are presented as typical examples for these substrates. The patterns are dominated by an intense FAD radical signal. A poorly resolved Mo(V) species and the broad FeS signal always appear with much larger relative intensity in the anaerobic sample compared to the aerobic preparation. In case of isoquinoline, an anaerobical sample in D_2O was successfully prepared. The resulting Mo(V) signal, which is shown in the insert of trace d*, has a clearly reduced overall line width. Trials to isolate the Mo(V) species by subtraction of spectra obtained under anaerobic and aerobic conditions for the various substrates yielded rather noisy, only poorly resolved patterns (data not shown) with essentially axial symmetry from which the **g** tensor components were estimated (Table 1). In this context, it should be mentioned that the preparation of samples in D_2O with a sufficient concentration of the rapid species so far was successful only for the isoquinoline-treated batch, because of the general sensitivity to residual traces of oxygen.

An interesting observation is made for the aerobically prepared sample with isoquinoline added (Figure 6e), which shows two features, $\mathbf{g} = 1.945$ and 1.935, similar to those of the aerobic enzyme incubated with quinaldine, but with larger intensity (trace e* is enhanced by a factor of 4). A close inspection also reveals an additional peak in the flank of the FAD radical at **g** factor of 2.024, which is marked with an arrow (Figure 6e). The **g** factors of this pattern closely correspond to those of the very rapid species in QuinOr and XanOx (Table 1). A Mo(V) signal corresponding to a resting species could not be isolated spectroscopically.

In dithionite-reduced enzyme, a broadened distinct axial EPR signal of an iron-sulfur center (FeSIax) appeared at 77 K, which gained resolution and intensity at lower temperatures. In addition, a second FeS center (FeSII) with rhombic symmetry was detectable below 60 K (Figure 6f). This is at variance with the findings for QuinOr and IsoOr for which all centers provided rhombic symmetry. No indications for a magnetic interaction between clusters were observed for variation in temperature or different amounts of reductant added.

Potentiometric Determination of Redox Potentials. Redox Properties of Iron-Sulfur Centers. In Figure 7, some representative EPR spectra of redox series of the three enzymes, poised at characteristic redox potentials and measured at 25 K, are compiled to indicate which of the signals of the FeS centers could be used for an analysis. For QuinOr, the signals I_2 and II_2 are severely overlapping with mediator (mainly from viologen dyes) and Mo(V) rapid q signals in a wide range of applied potentials, but the other components are sufficiently free to be analyzed (Figure 7, spectra a and b). In case of QualOx at low potentials, the mediator signal prevents an evaluation of the I_{ax1} and the II_2 component (Figure 7c). At the rather high potential of −80

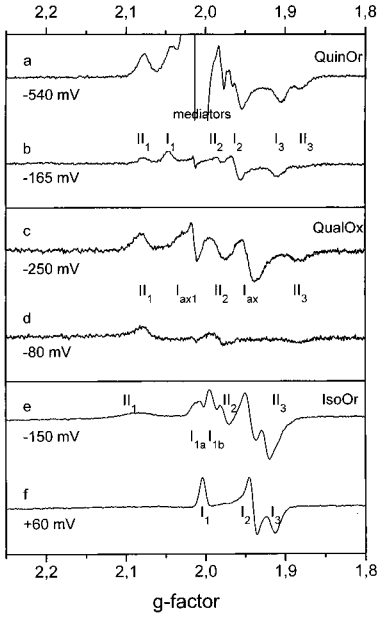

FIGURE 7: EPR spectra of the FeS centers of QuinOr (a, b), QualOx (c, d), and IsoOr (e, f) obtained at various redox potentials. Spectrum a illustrates the overlap of intense mediator signals at low potentials, spectra c and d indicate the large difference between both midpoint potentials of both FeS centers in QualOx. Spectra e and f illustrate the loss of the splitting of FeSI1 of IsoOr with oxidation of FeSII. All spectra were recorded at 25 K with 0.4 mT modulation amplitude.

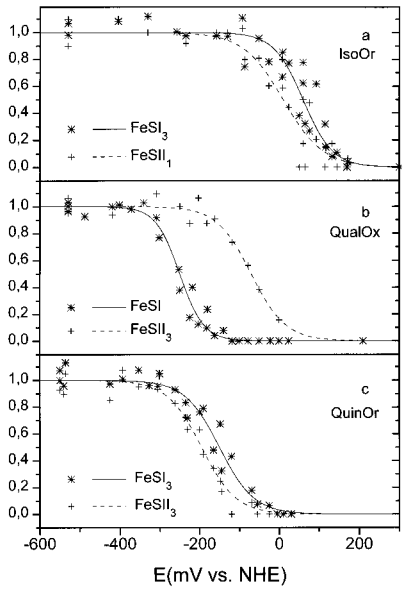

FIGURE 8: Behavior of the reduced FeS centers of IsoOr (a), QualOx (b), and QuinOr (c) in potentiometric titration in Tris-HCl buffer at pH 8.0. The degree of reduction is plotted as a function of potential with respect to the standard hydrogen electrode. The theoretical curves represent the amount of reduced species formed in a single $n = 1$ reduction process with midpoint potential E_M; the straight lines are calculated for FeSI, the dotted lines for FeSII centers. Best fit values for the midpoint potentials are given in Table 3.

mV, no traces of the axial FeS species are detectable, whereas the FeSII signals are clearly present (Figure 7d). In IsoOr, particularly, the FeSI center is quite difficult to analyze: I_1 is split into two components and I_2 and I_3 are partially overlapping with signals of FeSII (Figure 7e). In the course of reduction, the purely rhombic spectrum at high potential (Figure 7f) develops the splitting simultaneously with the appearance of the signals of the FeSII center, thus confirming the presence of a dipolar interaction between the FeS centers already suggested from partial reduction experiments.

For all accessible signals of each center (see Materials and Methods), the fitting to the Nernst-equation was performed and subjected to a statistical analysis. In Figure 8, the intensities of those FeS signals are plotted as a function of the redox potential, which provided the best Pearson coefficient of correlation R (see Table 3). The potentials are given relative to the standard hydrogen electrode (NHE). All iron-sulfur centers showed single reduction processes. Because of full reduction, the mean intensities at low potential spectra are set to 1.0. Due to the logarithmic expression in the Nernst formula, only points ±150 mV around the midpoint potentials were used for calculation.

In Table 3, the calculated midpoint potentials E_M are compared for the three enzymes. The uncertainty in measurements of redox potentials, due to electrode errors, curve-fitting, traces of oxygen, and possible interference from mediators is estimated with ca. ±15 mV, for IsoOr, ±30 mV. The worse correlation of regression data for IsoOr is also reflected by the lower values of the Pearson coefficient of correlation R, especially for iron-sulfur center II. This effect may be due to the more pronounced overlap of signals in the spectra of IsoOr (Figure 7). However, it was also noticed, that equilibration after dithionite addition took more time (up to 20 min) for samples of IsoOr than for the other two enzymes, for which about 5 min were sufficient.

In QuinOr, the midpoint potentials are relatively close to each other (Figure 8a, Table 3). In contrast, for QualOx the difference between both midpoint potentials is remarkably high (Figure 8b). While the axial species FeSI possesses a potential comparable to other investigated molybdenum hydroxylases, the potential of FeSII is about 180 mV higher. It is also noted that the sequence of potentials is reversed for FeSII and FeSI in comparison with the other two enzymes. The midpoint potentials determined for IsoOr are astonishingly high (in the positive millivolt range) and may characterize the outstanding position of this enzyme in the row of molybdenum hydroxylases (Table 3, Figure 8c).

All titration curves showed a less steep slope as required for ideal behavior. Regression analysis with the Nernst factor f_N as regressor yielded values greater than 59 mV (Table 3), which leads to a number of exchanged electrons of less than 1. For QuinOr, IsoOr, and the FeSII center of QualOx, the P value is smaller than the significance level of 0.05, so that the alternative hypothesis $f_N > 59$ mV is statistically proven, whereas for the FeSI center of QualOx the alternative hypothesis cannot be proven to the significance level.

Redox Properties of Molybdenum Centers. Figure 9, spectra a−d, shows the normalized spectra of the rapid q species in QuinOr recorded at 77 K at four potentials. The largest signal intensity was monitored around −390 mV (Figure 9b). The appearance of a maximum for the rapid q species is typical for a two single electron reduction process and correlated to the redox couples Mo(VI)/Mo(V) and Mo(V)/Mo(IV). The value of −390 mV corresponds to the mean potential $E_{mean} = 0.5(E^{Mo(VI)/Mo(V)} + E^{Mo(V)/Mo(IV)})$ of both redox processes. A quantitative determination of the single redox potentials was not performed, because previous determinations on XanOx at physiological pH values yielded differences within the error range of measurement (Cammack et al., 1976; Hille, 1996). For all efforts, trying a wide range of redox potentials, different temperatures, and annealing

Table 3: Redox Properties of the Iron-Sulfur Centers

	QuinOr FeSI	QuinOr FeSII	QualOx FeSI	QualOx FeSII	IsoOr FeSI	IsoOr FeSII
E_M (vs NHE) (mV)	−155	−195	−250	−70	65	10
f_N (mV)	100	100	70	105	85	115
R	0.9583	0.9735	0.9589	0.9856	0.8769	0.9093
P value	0.0013	0.0020	0.0975	0.0071	0.0278	0.0044

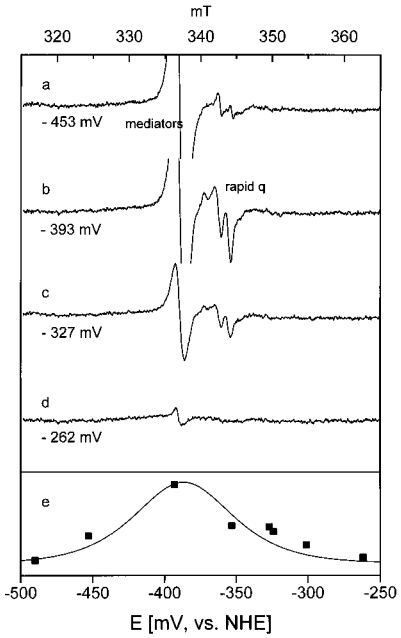

FIGURE 9: Behavior of the Mo(V) rapid EPR signal (a−d) of QuinOr in potentiometric titration in Tris-HCl-buffer at pH 8.0. In spectrum e, the intensity of the Mo(V) signal is plotted as a function of potential with respect to the standard hydrogen electrode. The straight line presents best-fit curves for the amount of Mo(V) formed in a consecutive $n = 1$ reduction process with midpoint potential E_M. All spectra were recorded at 77 K with 0.4 mT modulation amplitude.

samples, no Mo(V) signals could be produced in IsoOr and QualOx.

DISCUSSION

In continuation of our work on QuinOr, the variety of signal giving species, obtained upon reduction with dithionite or substrate, could be characterized in more detail by isotope substitution and spectra simulation. In addition, further species were detected. A significant finding is the induction of the rapid q signal upon reduction with dithionite, contrasting previous results (Tshisuaka et al., 1983). Consequently, a suggested catalytical relevance of the rapid q species is less probable. The assumption is fortified by the fact that addition of substoichiometric portions of substrate does not produce the rapid signal, so that its occurrence has to be related to the presence of reduced Mo(V) enzyme in the sample. This is in agreement with kinetic studies of XanOx (Hille, 1994), which prove, that the rapid species does not constitute an intermediate of the catalytical process, but a reduced form of the molybdenum center with inhibitory influence on the enzyme turnover. The small variation of proton hyperfine splitting in dithionite reduced samples compared to substrate addition (Table 1) is indicative for a slightly altered geometry or spin distribution of the Mo(V) complex, but does not necessarily require direct binding of quinoline. Enrichment of the enzyme with ^{95}Mo ($I = {}^5/_2$) was performed to elucidate the molybdenum hyperfine tensor. Simulations of the rapid q signal of ^{95}Mo-enriched samples yielded a slight rhombicity of the **g** tensor and a rhombic ^{95}Mo hyperfine tensor. Best agreement with experimental pattern was achieved by introducing a noncollinearity of 25° between the principal axes of the maximal components. A similar deviation from collinearity (18°) was also obtained for simulations of the rapid species in XanOx isotopically enriched in ^{95,97}Mo (George & Bray, 1988). It is indicative of signal-giving Mo center with C_{2v} symmetry.

Simultaneous addition of the substrate quinoline and the nonsubstrate quinaldine to QuinOr leads to the detection of the very rapid q species, for which, by simulation, comparable **g** factors as for the very rapid species of XanOx were found. Obviously, the competition between the substrate and quinaldine expands the time scale for the formation of the catalytic intermediary very rapid species to accumulate in sufficient concentration. In order to detect the very rapid species without such an inhibiting effect, rapid-freeze techniques, as employed with XanOx, (Gutteridge & Bray, 1978a,b) will be necessary.

In the desulfo form of the enzyme, prepared by treatment with cyanide, a Mo(V) signal with typical properties of a slow species appeared upon reduction with dithionite. Refined spectral isolation and simulations revealed nearly axial symmetry and an exchangeable proton coupling. In unreduced desulfo samples, a second inactive resting species can be isolated, which is probably induced by the process of inactivation.

Redox titrations of QuinOr revealed a midpoint potential of about −390 mV for the Mo center, which is well in line with those of other members of the xanthine oxidase family. Corresponding values for XanOx determined by EPR range from −315 (Porras & Palmer, 1982) to −377 mV (Barber & Siegel, 1982), depending on the conditions of measurement (temperature, buffer, pH value). The lowest redox potential for a molybdenum center, reported so far, is that of aldehyde oxidoreductase from *Desulfovibrio gigas*, which amounts to −450 mV [Mo(VI)/Mo(V)] and −530 mV [Mo(V)/Mo(IV)] (Barata et. al., 1993). On the whole, the signal giving Mo(V) species in QuinOr is similar to a great extent to those in XanOx. In particular, evidence of the very rapid species implies that mechanistic models discussed for XanOx may also apply to QuinOr. It is also noteworthy, that the rapid q species, albeit considered to be catalytically not relevant, may serve as a sensitive monitor of the paramagnetic Michaelis complex (Hille, 1996) in, for example, genetically modified enzymes.

In QualOx, an essentially axial Mo(V) rapid signal with low spectral resolution was found under anaerobic conditions. When oxygen [the final electron acceptor of the enzyme (Stephan et al., 1996)] was allowed, mainly an anionic FAD radical species was present, but also traces of a very rapid species could be detected for the substrates quinaldine and isoquinoline. With these substrates, QualOx shows relative activities of 100% and 200%, respectively. Other types of substrates which were employed so far, i.e., quinoline and 2-chloroquinoline, which are converted with relative activities

of about 300% and 500%, did not yield detectable amounts of very rapid signals. They seem to have escaped detection, because of a much faster kinetic behavior as compared to quinaldine or isoquinoline. In dithionite reduced QualOx, a distinct axial EPR signal of an FeS center ($FeSI_{ax}$) appeared already at 77 K, gaining intensity at lower temperatures, a second FeS center with rhombic symmetry was detectable below 60 K. This is at variance with the findings for QuinOr and IsoOr for which all centers provided rhombic symmetry. The pronounced axiality of the $FeSI_{ax}$ center in QualOx can be associated with a more symmetrical cysteine−ligand arrangement at the iron-sulfur cluster as compared to the other enzymes.

IsoOr shows significant differences in the behavior of Mo(V) signals to QuinOr. On reduction with substrate, the very rapid i species arises immediately after addition, remaining stable for a prolonged time. On the other hand, the rapid i signal is first observed after a few min and vanishes within 10 min. These findings are in clear contrast to XanOx or QuinOr and indicative for differences in the kinetics of signal formation. Probably, the very rapid i signal originates from an inhibitory species. Such a persisting signal was also found upon addition of alloxanthine to XanOx (Hawkes et al., 1984), which was interpreted as an inhibitory complex. At present, it only can be suggested that the absence of FAD and the final electron acceptor in samples of IsoOr is responsible for the formation of an inhibited state. Clearly, further studies in the fast time regime and in the presence of artificial substitutes of the unknown physiological electron acceptor are required to clarify the unusual behavior of Mo(V) species in IsoOr.

A surprising result was the absence of any Mo(V) signals in redox titrations of QualOx and IsoOr, which, in contrast, were readily observed for QuinOr. A plausible explanation is offered by a direct reduction of Mo(VI) to the EPR silent Mo(IV) state under the experimental conditions applied, which is in line with the presence of only very small amounts of Mo(V) signals in concentrated samples of both enzymes upon reduction with dithionite. A determination of the Mo redox potentials may be feasible by changing to different buffer systems and/or pH values.

In analogy to XanOx and QuinOr, two rhombic iron-sulfur signals arise after reduction of IsoOr with substrate or dithionite. At temperatures below 50 K, a prominent splitting of the $FeSI_1$ line is appearing, whereas smaller effects are deduced from simulations for $FeSI_2$ and I_3 (see Table 2). The lines of FeSII are quite broad, but do not show a resolved splitting. Because no Mo(V) signals are observable in the spectrum and the split feature is also obtained in the course of redox titration, a magnetic interaction between both FeS centers is assumed to be responsible for the splitting. In this context, IsoOr shows similarities to aldehyde oxidoreductase of *D. gigas*, in which the $\mathbf{g}_1$ feature of FeSI is also resolved into two features under some conditions (Bray et al., 1991; Moura et al., 1978). However, in this case the authors also discuss a possible influence of Mo(V) on the splitting in analogy to the observation of magnetic interaction of the Mo(V) site and the FeS center studied for xanthine oxidase (Lowe et al., 1972; Lowe & Bray, 1978), which can be excluded in our case, since the splitting can be observed in the absence of Mo(V). For a purely dipolar interaction (e.g., no exchange contributions), a maximum distance of ca. 15 Å between the two FeS centers is estimated from the maximal splitting of 3.0 mT applying the simple point dipole approximation. However, one has to bear in mind that this approach is neglecting noncollinear arrangement of the dipole moments as well as the delocalization of magnetic moment over the spatially extended clusters and their individual electronic structure. Recently, it has been successfully shown that detailed structural information can be obtained by applying local spin vector models to simulate spectra of dinuclear (or polynuclear) centers interacting with mononuclear centers or other polynuclear centers (Bertrand et al., 1994, 1995, 1996). For IsoOr, more reliable values for the distance between the two FeS centers are expected by using the more elaborate method. The estimated value can be compared with the center to center distance of 13.4 Å between the FeS clusters in the X-ray structure of the *D. gigas* aldehyde oxidoreductase (Romaõ et al., 1995). At the moment, it only can be supposed that the corresponding distance in IsoOr may even be shorter or that the relative arrangement of clusters may be considerably different.

The most significant differences between the three studied enzymes refer to the redox properties of the iron-sulfur clusters. For QuinOr, which shows numerous similarities to other molybdenum hydroxylases, potentials of −155 mV for FeSI and −195 mV for FeSII were inferred in low-temperature measurements. These values have to be compared to the midpoint potentials for FeSI/FeSII in XanOx [−343/−303 mV (Cammack et al., 1976), −310/−217 mV (Porras & Palmer, 1982), and −310/−255 mV (Barber & Siegel, 1982)], chicken liver xanthine dehydrogenase [−295/−292 mV (Barber et al., 1977) and −280/−275 mV (Barber et al., 1980)], milk xanthine dehydrogenase [−310/−235 mV (Hunt et al., 1993)], and rabbit liver aldehyde oxidase [−207/−310 mV (Barber et al., 1982)]. It is noted that the assignment of the high and low redox potentials to centers I and II is reversed in relation to, e.g., XanOx. In addition, the midpoint potentials are generally more positive compared with the other enzymes. Analysis of the redox data of QualOx yielded widely separated midpoint potentials of −250 mV for FeSI and −70 mV for FeSII. In this case, the assignment of low and high redox clusters is again like in XanOx. Most striking, however, are the high redox potentials of the iron-sulfur centers of IsoOr (10 mV for FeSII, 65 mV for FeSI), again with a reversed assignment in comparison to XanOx. To our knowledge, positive redox potentials for both FeS centers have not been reported for other enzymes of the xanthine oxidase family. The reason for these unusual potentials and a possible relation to the unknown physiological electron acceptor has to remain the object of further studies.

An interesting detail of redox studies is the decreased slope of the titration curves, which is most pronounced for QuinOr and IsoOr. Cammack et al. (1976) observed a similar effect on titration of XanOx in pyrophosphate buffer, whereas in Tris buffer, redox behavior was essentially ideal. Because of this difference, the nonideal behavior was ascribed to heterogeneity in the enzyme molecules, probably as a result of binding of buffer molecules. To explain the observations in our experiments, two possibilities are discussed not requiring effects of buffer binding.

In the case of IsoOr, where EPR spectra indicate a dipolar interaction between both FeS clusters due to spatial proximity, negative cooperativity may play a role. When two redox centers A and B show negative cooperativity, then the reduction of A shifts the midpoint potential of B to more negative values and vice versa. If the spectra of the

intermediary species A^-B and AB^- can be monitored independently of AB and A^-B^-, then the titration curves can be simulated with two redox potentials for each cluster (Cammack, 1994). The alternative approach is based on the observation of pronounced strain effects, which become visible in large EPR line widths in X- and Q-band experiments as well as in broadened ENDOR resonances in enzyme samples. Correlating these effects to a distribution in structural and electronic properties of the paramagnetic centers, a distribution of midpoint potentials was introduced in the Nernst equation, which originally is deduced for redox centers with identical thermodynamic properties. Depending on the distribution of individual midpoint potentials, expressed in the value of the standard deviation σ, the slope of the redox curve decreases. For example a σ value of 40 mV results in a titration curve with a Nernst factor f_N of approximately 80 mV approaching the values listed in Table 3. If, additionally, negative cooperativity is involved, then the decrease of the slope (or the increase of f_N) is further enhanced, so that both effects cannot be separated from each other. The distribution of midpoint potentials might well be modulated by a structural flexibility of protein domains, in which the redox active center is located and may be of importance for its functional role.

REFERENCES

Barata, B. A. S., LeGall, J., Moura, J. J. G. (1993) *Biochemistry 32*, 11559−11568.

Barber, M. J., & Siegel, L. M. (1982) *Biochemistry 21*, 1638−1647.

Barber, M. J., Bray, R. C., Cammack, R., & Coughlan, M. P. (1977) *Biochem. J. 163*, 270−289.

Barber, M. J., Coughlan, M. P., Kanda, M., & Rajagopalan, K. V. (1980) *Arch. Biochem. Biophys. 201*, 468−475.

Barber, M. J., Coughlan, M. P., Rajagopalan, K. V., & Siegel, L. M. (1982) *Biochemistry 21*, 3561−3568.

Bauder, R., Tshisuaka, B., & Lingens, F. (1990) *Biol. Chem. Hoppe-Seyler 371*, 1137−1144.

Bertrand, P., More, C., Guigliarelli, B., Fournel, A., Bennet, B., & Howes, B. J. (1994) *J. Am. Chem. Soc. 116*, 3078−3086.

Bertrand, P., More, C., & Camensuli, P. (1995) *J. Am. Chem. Soc. 117*, 1807−1809.

Bertrand, P., Camensuli, P., More, C., & Guigliarelli, B. (1996) *J. Am. Chem. Soc. 118*, 1426−1434.

Bläse, M., Brunther, Ch., Tshisuaka, B., Fetzner, S., & Lingens, F. (1996) *J. Biol. Chem. 271*, 23068−23079.

Bray, R. C. (1975) in *The Enzymes* (Boyer, P. D., Ed.) pp 300−419, Academic Press, New York.

Bray, R. C. (1980) *Adv. Enzymol. Relat. Areas Mol. Biol. 51*, 107−165.

Bray, R. C. (1988) *Q. Rev. Biophys. 21*, 299−329.

Bray, R. C., & Swann, J. C. (1972) *Struct. Bonding 11*, 107−144.

Bray, R. C., Gutteridge, S., Stotter, D. A., & Tanner, S. J. (1979) *Biochem. J. 177*, 357−360.

Bray, R. C., Turner, N. A., LeGall, J., Barata, B. A. S., & Moura, J. J. G. (1991) *Biochem. J. 280*, 817−820.

Cammack, R. (1994) in *Bioenergetics: a Practical Approach* (Brown, G. C., Cooper, C. E., Eds.) pp 85−109, IRL Press, Oxford.

Cammack, R., Barber, M. J., & Bray, R. C. (1976) *Biochem. J. 157*, 469−478.

Coughlan, M. (1980) in *Molybdenum and Molybdenum-containing Enzymes* (Coughlan, M., Ed.) pp 119−185, Pergamon Press, Oxford.

Cramer, S. P. (1983) in *Advances in Inorganic and Bioinorganic Mechanisms* (Sykes, A. G., Ed.) pp 259−315, Academic Press, London.

George, G. N., & Bray, R. C. (1988) *Biochemistry 27*, 3603−3609.

Gutteridge, S., & Bray, R. C. (1980a) in *Molybdenum and Molybdenum-containing Enzymes* (Coughlan, M., Ed.) pp 223−239, Pergamon Press Oxford.

Gutteridge, S., & Bray, R. C. (1980b) *Biochem. J. 189*, 615−623.

Gutteridge, S., Tanner, S. J., & Bray, R. C. (1978a) *Biochem. J. 175*, 869−878.

Gutteridge, S., Tanner, S. J., & Bray, R. C. (1978b) *Biochem. J. 175*, 887−897.

Hawkes, T. R., George, G. N., & Bray, R. C. (1984) *Biochem. J. 218*, 961−968.

Hille, R. (1994) *Biochim. Biophys. Acta 1184*, 143−169.

Hille, R. (1996) *Chem. Rev. 96*, 2757−2816.

Hille, R., & Massey, V. (1985) in *Molybdenum Enzymes* (Spiro, T. G., Ed.) pp 443−517, J. Wiley and Sons, Inc., New York.

Hunt, J., Massey, V., Dunham, W. R., & Sands, R. H. (1993) *J. Biol. Chem. 268*, 18685−18691.

Iwasaki, M. (1974) *J. Magn. Reson. 16*, 417−423.

Johnson, J. L., Rajagopalan, K. V., & Meyer, O. (1990) *Arch. Biochem. Biophys. 283*, 542−545.

Lehmann, M., Tshisuaka, B., Fetzner, S., Röger, P., & Lingens, F. (1994) *J. Biol. Chem. 269*, 11254−11260.

Lehmann, M., Tshisuaka, B., Fetzner, S., & Lingens, F. (1995) *J. Biol. Chem. 270*, 14420−14429.

Lowe, D. J., & Bray, R. C. (1978) *Biochem. J. 169*, 471−479.

Lowe, D. J., Lynden-Bell, R. M., & Bray, R. C. (1972) *Biochem. J. 130*, 239−249.

Massey, V., & Edmondson, D. (1970) *J. Biol. Chem. 245*, 6595−6598.

Moura, J. J. G., Xavier, A. G., Cammack, R., Hall, D. O., Bruschi, M., & Le Gall, J. (1978) *Biochem. J. 173*, 419−425.

Palmer, G., Müller, F., & Massey, V. (1971) in *Flavins and Flavoproteins* (Kamin, H., Ed.) pp 123−140, University Park Press, Baltimore.

Pilato, R. S., & Stiefel, E. I. (1993) in *Bioorganic Catalysis* (Reedijk, J., Ed.) pp 131−188, Marcel Dekkar, Inc., New York.

Porras, A. G., & Palmer, G. (1982) *J. Biol. Chem. 257*, 11617−11626.

Romaõ, M. J., Archer, M., Moura, I., Moura, J. J. G., LeGall, J., Engh, R., Schneider, M., Hof, P., & Huber, R. (1995) *Science 270*, 1170−1176.

Stephan, I., Tshisuaka, B., Fetzner, S., & Lingens, F. (1996) *Eur. J. Biochem. 236*, 155−162.

Tshisuaka, B., Kappl, R., Hüttermann, J., & Lingens, F. (1993) *Biochemistry 32*, 12928−12934.

BI970581D